Ab Initio Study of the Most Stable C_4H_5 Isomers

C. L. Parker and A. L. Cooksy*

Department of Chemistry, University of Mississippi, University, Mississippi 38677

Received: November 24, 1998; In Final Form: January 25, 1999

Ab initio calculations have been carried out on the lowest energy isomers of C_4H_5 to predict spectroscopic properties and relative stabilities. Geometry optimizations were carried out on stationary point conformations of seven configurational isomers at UHF, B3LYP, MP2, CISD, QCISD, MCSCF(7,7), and MCSCF(9,9) levels of theory. Single-point energies were evaluated at the MP4, CCSD(T), MCSCF(11,11), and multireference CISD levels. Disparities as large as 70 kJ mol^{-1} are found between relative energies predicted by single- and multireference methods for the same isomer. Comparison to experimental values suggests that the multireference methods inadequately model the relative correlation energy. Zero-point corrected relative energies (in kJ mol^{-1}) obtained at the QCISD level with a 6-311G(d,p) basis set are the following: 2-butyn-1-yl (0); 1-butyn-3-yl (10); 1,2-butadien-4-yl (13); cyclobuten-3-yl (17); 1,3-butadien-2-yl (50); 1,3-butadien-1-yl (59); and 1-butyn-4-yl (64). Relative energies calculated by multireference methods are higher, and decrease slowly as the active space size increases. Relative energies and hyperfine constants obtained at the QCISD level are in agreement with available experimental data and empirical estimates. Some of these isomers are candidates for relocalization, a phenomenon that results in predicted multiple minima and unusually flat vibrational potential energy surfaces for the isoelectronic C_3H_3O isomers. Of the present series of molecules, only 2-butyn-1-yl exhibits an especially flat bending potential along the appropriate isomerization coordinate. Predicted vibrational transition frequencies and intensities, dipole moment components, Fermi contact hyperfine constants, and conformational potential energy curves are presented.

1. Introduction

Several C_4H_5 radical isomers are important intermediates in the pyrolysis[1−9] and photochemistry[10−12] of unsaturated hydrocarbons, and are candidates for detection in the interstellar medium.[13] Various C_4H_5 isomers have been under investigation since 1967, when Martin and Sanders measured the kinetics of perester decomposition to radical products[14] and Benson and Haugen included the 1,3-butadienyl radicals in their kinetic model of radical-mediated carbon chain formation.[15] Subsequent kinetics studies have probed the role of these radicals in the photolysis of 2-butyne,[10] the thermal decomposition of pentyne and pentadiene,[1,2] the pyrolysis of 1-butyne[3] and 1,2-butadiene,[8] and the radical-mediated chain formation leading to aromatic compounds.[4−7,9,11,12,16] Several of these studies have succeeded in predicting formation enthalpies for the more stable C_4H_5 isomers. There are also many ESR measurements of the magnetic and hyperfine properties of selected C_4H_5 isomers.[17−22] An elegant crossed-beam study by Kaiser and co-workers has recently probed the mechanism for formation of several of these structures from the reaction of propene and atomic carbon.[23] Selected structural isomers have been the subject of previous studies by ab initio and semiempirical theory,[24−26] including several studies of the higher energy cyclic and bicyclic structures.[27−29]

The C_4H_5 radicals are isoelectronic with the C_3H_3O radicals, one methylene group being replaced by an oxygen atom. Several of the C_3H_3O structural isomers present multiple nonequivalent canonical geometries that differ by "relocalization", an isomerization pathway that exchanges the formal locations of an unpaired electron and one end of a neighboring π bond. In particular, the H_2C_2HCO, H_2C_3HO, and H_3C_3O radicals were found to have very flat ab initio potential surfaces along the relocalization bending coordinate.[30] Similar results have also been obtained for the glyoxallyl radical OCCHO.[31] The relocalization pathways in these species connect two configurations with different electronic state symmetries, usually requiring the isomerization to break the molecular point group symmetry. This contrasts with the relocalization pathways found for the C_3HO and C_4H_3 radicals,[32,33] which convert one $^2A'$ configuration into another on a C_s isomerization surface.

Canonical geometries for the most stable C_4H_5 radicals are presented in Figure 1. Among these formal geometries, there are three pairs which interconvert by relocalization: $H_3C_4H_2$ with configurations 2-butyn-1-yl (1a) and 1,2-butadien-3-yl (1b and 2), HC_3HCH_3 with configurations 1-butyn-3-yl (3a) and 1,2-butadien-1-yl (3b), and $H_2C_3HCH_2$ with configurations 1,2-butadien-4-yl (4) and 1,3-butadien-2-yl (5).

Despite many previous experimental and theoretical studies of these isomers, an ab initio study of the global C_4H_5 potential energy surface has not been reported since the exhaustive series of relative energies calculated at the UHF and MP3 levels by Somasundram.[34] The primary goal of the present work is to predict the spectroscopic and thermodynamic properties of the most stable C_4H_5 isomers by high-level ab initio methods, taking advantage of recent experimental data to assess the results.

We have previously presented results of QCISD and MCSCF-(9,9) calculations on the radicals obtained by hydrogen atom abstraction from 1,3-butadiene.[35] This family of C_4H_5 isomers consists of the $H_2C_3HCH_2$ and H_2C_2HCHCH radicals drawn in Figure 1. In the current report we place those calculations in the context of the global C_4H_5 surface, and present additional

* Author to whom correspondence should be addressed.

10.1021/jp984535e CCC: $18.00
Published on Web 03/11/1999

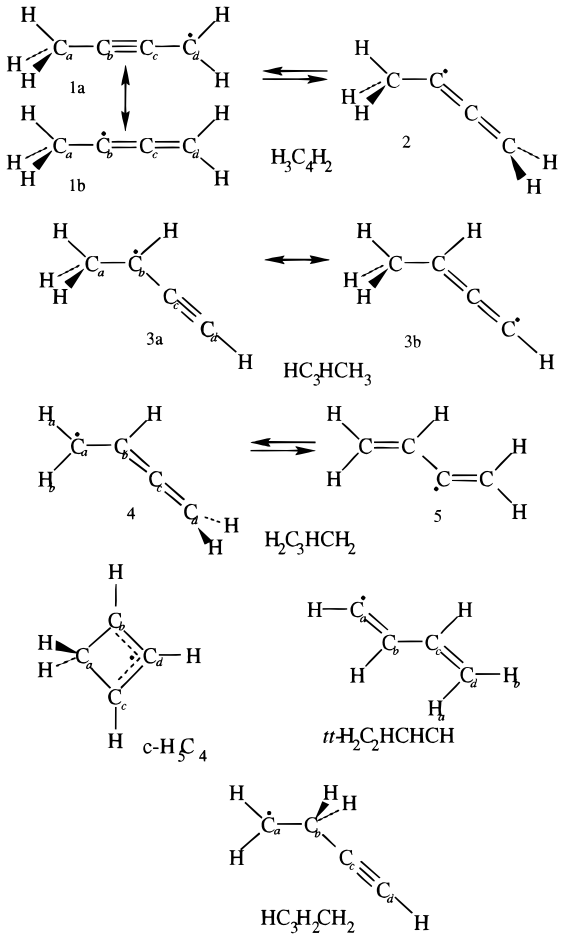

Figure 1. Canonical structures of the principal C_4H_5 isomers studied.

results for these isomers without altering the conclusions of the previous work.

2. Methods

Structural and configurational isomers of C_4H_5 were initially selected by considering single hydrogen abstractions from the closed-shell C_4H_6 isomers. Three radicals are derived from 1-butyne, one from 2-butyne, two from 1,3-butadiene, and three from 1,2-butadiene. Cyclic structures consisted of the two radicals formed from cyclobutene, two from bicyclobutane, five from 1- and 3-methylcyclopropene, and two from methylenecyclopropane. Altogether, 20 distinct geometries were examined. Of these, six pairs share a common isomeric structure (such as configurations 4 and 5 in Figure 1).

An initial survey of the C_4H_5 structural isomers was carried out at the UHF level using a 6-311G(d,p) basis set,[36,37] which has been shown to be well-converged for similar unsaturated carbon-chain free radicals.[31,32] For the C_4H_5 isomers, this basis set encompasses 102 contracted Gaussian functions. The energy of the optimized cyclic H_5C_4 structure relative to the most stable structure is reported in Table 1 for several basis sets, including Dunning's correlated basis sets with double and triple-ζ functions,[38] the largest of which nearly doubles the number of contracted basis functions. The single most important contribution to the basis set is clearly the use of d polarization functions on the carbons; no increase in the basis set size thereafter alters the relative energy by more than 12 kJ mol^{-1}. Although Tao and Pan have demonstrated that the effect of polarization functions can be achieved more efficiently through use of mid-bond functions in cases of long bond lengths,[39] Partridge and Bauschlicher recently established that mid-bond functions do not accelerate the convergence of electronic wave functions for typical covalent bonds.[40]

TABLE 1: QCISD Relative Energy of Cyclic H_5C_4 as a Function of Basis Set

basis	number of functions	ΔE [kJ mol^{-1}]
6-31G	46	51.9
6-311G	67	53.8
cc-pVDZ	81	6.7
6-31G(d,p)	85	9.1
6-311G(d)	87	15.1
6-311G(d,p)	102	12.4
6-311G(2d,2p)	137	18.2
cc-pVTZ	190	12.2

The UHF survey confirmed qualitative results obtained previously by Somasundram[34] using smaller bases. The isomers selected for further study in this work are only the six most stable structural isomers of C_4H_5 as determined by this survey. These six isomers account for all the C_4H_5 minimum energy geometries within 100 kJ mol^{-1} of the global minimum on the UHF potential surface. Somasundram carried out MP3/6-31G(d) calculations on the 10 lowest energy structural isomers, finding these same six isomers to be the lowest energy, their stabilization energies within 80 kJ mol^{-1} of each other. The seventh most stable isomer appears to be the 1-methylylcyclopropene radical, some 10 to 20 kJ mol^{-1} higher in energy as determined by UHF and Somasundram's MP3 calculations.

In our studies of the isoelectronic C_3H_3O and OCCHO isomers,[30,31] occasional disparities of up to 30 kJ mol^{-1} have been found between those relative energies predicted by methods based on a single UHF reference wave function and those predicted by multireference methods. The disparities are resolved by extending the multiconfiguration calculations, either by expansion of the active spaces or by addition of a truncated CI series of single and double substitutions to higher energy virtual orbitals. Relative energies predicted by single- and multireference methods eventually converge to within 15 kJ mol^{-1}. Nevertheless, the high spin contamination found in these calculations dictates that a multiconfiguration analysis remains prudent.

We have therefore employed several different approximation methods for estimation of the correlation energy. The post-SCF levels of theory described in this report include MP2, complete active space multi-configuration SCF (MCSCF),[41,42] single-reference configuration interaction with single and double substitutions (CISD),[43] quadratic CISD (QCISD),[44] and the CCSD(T) coupled cluster method.[44] The QCISD equations are themselves truncated CCSD equations,[45] and tend to predict results very similar to those obtained at the CCSD(T) level. In comparison of ab initio predictions to spectroscopic data for HC_3O,[32] it was found that QCISD adequately predicted hyperfine constants and vibrational frequencies. Barone and coworkers have also found that the QCISD method in conjunction with a triple-ζ basis set accurately reproduced experimental hyperfine constants for bicyclic C_4H_5 isomers.[22]

Of the parameters reported in the C_3H_3O and butadienyl studies, only the relative energies and hyperfine constants were profoundly affected by the level of theory.[30,35] Equilibrium geometries, harmonic vibrational frequencies, and dipole moments are found to change little from high-level single-reference to multireference predictions.

Geometry optimizations were carried out on these six structural isomers at the B3LYP,[46,47] MP2,[48] CISD, QCISD, and MCSCF levels. Initial geometries for the optimizations were

TABLE 2: Absolute Energies (har) of $H_3C_4H_2$ and Zero-Point Corrected Relative Energies (kJ mol^{-1}) of the Most Stable C_4H_5 Configurational Isomers[a]

	$H_3C_4H_2$ (1) $^2A'$ *E*	HC_3HCH_3 (3) stag $^2A''$ ΔE	$H_2C_3HCH_2$ (4) $^2A''$ ΔE	$H_2C_3HCH_2$ (5) $^2A'$ ΔE	cyc-H_5C_4 $^2A_2$ ΔE	H_2C_2HCHCH *tt* $^2A'$ ΔE	$HC_3H_2CH_2$ $^2A''$ ΔE
UHF	−154.3333271	13.3	3.4	[20.3]	26.5	28.1	72.8
B3LYP	−155.3730879	15.3	6.0	[47.1]	34.6	63.7	84.9
MP2	−154.8523906	[15.0]	32.9	84.4	15.0	91.0	32.7
CISD	−154.8195209	13.6	17.2	[58.7]	14.0	66.3	57.2
QCISD	−154.9032563	**9.6**	**12.5**	**[50.2]**	**17.2**	**59.3**	**63.5**
MCSCF(7,7)	−154.4227758	[13.1]	56.9	75.0	84.0	83.2	51.4
MCSCF(9,9)	−154.4498167	12.4	47.5	76.6	89.0	84.7	61.0
MRCISD(7,7,43)[b]	−154.4767678	10.7	58.3	84.0	79.1	96.3	70.8
emp. (see text)		2(12)[1,57]	10(10)[5,8,57]		8(12)	65(9)	75(9)

[a] The basis set is 6-311G(d,p) for results from the present study in all tables. Relative energies for saddle point configurations are given in square brackets. [b] MRCISD zero-point corrections are estimated from the MCSCF(7,7) frequencies.

chosen to sample all the configurational isomers drawn in Figure 1. Configuration 2 of $H_3C_4H_2$ is not a stationary point on the UHF, QCISD, or MCSCF(9,9) surfaces of the ground electronic state, and was not investigated at other levels of theory.

We have previously shown that the cis conformer of $H_2C_3HCH_2$ configuration 5 is not stable, whereas four conformers of the H_2C_2HCHCH structure are minima on the potential energy surface.[35] Of the remaining four C_4H_5 structural isomers, the cyclic has only one conformer (having a C_{2v} geometry), whereas the $H_3C_4H_2$, HC_3HCH_3, and $HC_3H_2CH_2$ configurations each have two distinct C_s conformers. These conformers interconvert by torsion about a CC single bond, with any unique C_s structure necessarily corresponding to a stationary point (either a local minimum or maximum) along the torsional coordinate.

Active spaces in the MCSCF computations range in size from seven electrons in seven orbitals (7,7) to eleven electrons in eleven orbitals (11,11), with the orbitals selected so as to yield the lowest variational energy for a given molecular geometry. The active space orbitals generally comprise those occupied orbitals of the UHF reference corresponding to the π-bonds, CC σ-bonds, the singly occupied orbital, and those lowest energy unoccupied orbitals that balance the active space symmetry. For example, the optimal (11,11) active space for $^2A'$ $H_3C_4H_2$ consists of the three occupied CC σ-bond orbitals (all a' symmetry), the two π -bond orbitals (one a', one a''), the singly occupied orbital (a'), and the lowest energy set of four a' and one a'' unoccupied orbitals. However, in cases involving a straight HCCC chain, as in HC_3HCH_3 or $HC_3H_2CH_2$, the optimal active space replaces the off-axis CC bond orbital with the on-axis CH bond orbital. These choices were periodically tested by systematic calculation of the single-point energy for every unique permutation of the active space involving the occupied C−C bond and lowest five virtual orbitals; the selected active spaces always yielded the lowest variational energy of the set. The localization scheme of Pipek and Mazey[49] was used (subject to symmetry constraints) to simplify selection of the active space orbitals.

Relative energies are also calculated at the MP4,[50] CCSD(T),[44] MCSCF(11,11), and MRCISD levels using geometries optimized at lower levels of theory. For the isoelectronic OCCHO isomers, failing to optimize the geometries at these higher levels affects the relative energies by less than 5 kJ mol^{-1}.[31]

For C_s geometries, computational resources restricted a (7,7) active space MRCISD calculation to 43 external orbitals; this level of theory is denoted MRCISD(7,7,43) in Table 2. The MRCISD samples neither as extensive an active space as the MCSCF(11,11) calculations, nor as extensive a range of external orbitals as the CISD calculations, and is not necessarily superior to either method. However, MRCISD provides an avenue for incorporating into the wave function dynamical correlation effects which are typically under-sampled by MCSCF methods alone.

TABLE 3: Zero-Point Corrected Relative Energies (kJ mol^{-1}) of Stationary Point C_4H_5 Conformers[a]

	$H_3C_4H_2$ $^2A''-{}^2A'$	HC_3HCH_3 ecl−stag	$HC_3H_2CH_2$ $^2A-{}^2A''$	$HC_3H_2CH_2$ $^2A'-{}^2A''$
UHF	[0.1]	[1.6]	0.3	2.6
B3LYP	[0.0]	0.0	0.0	3.4
MP2	[0.0]	[0.3]	0.1	−0.5
CISD	[0.0]	[1.2]	0.2	2.3
QCISD	0.0	1.3	0.2	2.6
MCSCF(7,7)	0.0	[0.1]	0.7	1.9
MCSCF(9,9)	0.1	[0.9]	0.3	1.4

[a] Relative energies for saddle point configurations are given in square brackets.

The calculations were carried out on a variety of Silicon Graphics workstations and Cray supercomputers, using the Gamess 5.4 program set[51] for all multireference calculations and the Gaussian 94 program set[52] for all single-reference calculations.

3. Results and Discussion

For all geometry optimizations, the $^2A'$ conformer of $H_3C_4H_2$ is found to be the lowest energy point on the global C_4H_5 surface. Absolute energies of this conformer, predicted at several levels of theory, are reported in Table 2. For each of the remaining configurational isomers, Table 2 lists the relative energy of the most stable conformer, corrected for zero-point energy differences. The largest zero-point corrections are 4.0−5.5 kJ mol^{-1} for the cyclic structure; corrections for other structures are 3.5 kJ mol^{-1} or less. Relative energies of the stationary point conformations are given in Table 3 for $H_3C_4H_2$, HC_3HCH_3, and $HC_3H_2CH_2$. For each energy in Table 3, the zero-point correction includes all vibrational modes except the mode corresponding to the conformational isomerization. This gives relative energies on the effective potential energy curve for the isomerization.[32] A strict series of relative energies has not been determined for these isomers experimentally, and the quoted empirical values in Table 2 are discussed below for each configuration.

Table 4 lists the configurational energies (without zero-point correction) evaluated at several levels of theory, for the purpose of demonstrating convergence within various approximation methods. MP2 and MP4 relative energies agree to within 8 kJ mol^{-1} across all six structures, and Somasundram's MP3 energies agree within 10 kJ mol^{-1} of these for all but the cyclic structure; CISD, QCISD, and CCSD(T) results agree to within

TABLE 4: Energies (kJ mol^{-1}) of the Most Stable C_4H_5 Configurational Isomers Relative to $^2A'$ $H_3C_4H_2$

	HC_3HCH_3 (3) stag $^2A''$	$H_2C_3HCH_2$ (4) $^2A''$	$H_2C_3HCH_2$ (5) $^2A'$	cyc-H_5C_4 $^2A_2$	H_2C_2HCHCH *tt* $^2A'$	$HC_3H_2CH_2$ $^2A''$
MP2	13.3	31.7	78.9	13.0	86.2	37.0
MP3[34]	13.0	21.2		40.2	79.1	
MP4	12.6	26.5	74.9	13.2	82.2	45.0
CISD	12.9	17.0	56.8	10.2	63.9	59.3
QCISD	9.7	12.4	47.4	12.4	55.8	65.2
CCSD(T)	9.5	10.4	42.2	11.0	51.3	64.5
MCSCF(7,7)	13.1	58.6	73.7	78.9	81.0	53.8
MCSCF(9,9)	12.6	49.2	74.7	85.9	82.3	64.1
MCSCF(11,11)	10.0	41.5	62.2	79.9	71.2	64.6
MRCI(7,7,32)	3.3	54.6	72.4	55.9	83.4	70.0
MRCI(7,7,36)	12.0	56.3	87.4	73.7	94.7	71.8
MRCI(7,7,40)	11.4	55.4	78.3	69.0	86.2	71.4
MRCI(7,7,43)	10.7	60.0	82.7	74.0	94.1	73.2

TABLE 5: Values of $\langle S^2\rangle$, C_0^2, and Selected UNO Orbital Populations[a]

orbital	$H_3C_4H_2$	HC_3HCH_3	$H_2C_3HCH_2$	$H_2C_3HCH_2$	cyc-H_5C_4	H_2C_2HCHCH	$HC_3H_2CH_2$
$\langle S^2\rangle$	0.96	0.98	1.10	1.28	0.98	1.28	0.77
$\langle S^2\rangle_{ann}$[b]	0.78	0.79	0.84	0.91	0.76	1.18	0.75
C_0^2	0.91	0.65	0.46	0.89	0.78	0.79	0.90
UNO 6	1.9999	1.9999	1.9993	1.9995	1.9997	1.9996	2.0000
UNO 13	1.9654	1.9581	1.9087	1.9269	1.9962	1.9298	1.9986
UNO 14	1.9344	1.9293	1.8929	1.7362	1.8796	1.7283	1.9958
UNO 15	1.0000	1.0000	1.0000	1.0000	1.0000	1.0000	1.0000
UNO 16	0.0656	0.0707	0.1071	0.2638	0.1204	0.2717	0.0042
UNO 17	0.0346	0.0419	0.0913	0.0731	0.0038	0.0702	0.0014
UNO 24	0.0001	0.0001	0.0007	0.0005	0.0003	0.0004	0.0000

[a] $\langle S^2\rangle$ evaluated at QCISD optimized geometries; C_0^2 and UNO populations at MCSCF(9,9) optimized geometries. [b] $\langle S^2\rangle$ after annihiliation of spin contaminant.

13 kJ mol^{-1}; and MCSCF(7,7), (9,9), and (11,11) results agree to within 18 kJ mol^{-1}. The MRCISD relative energies appear relatively stable with respect to the number of external orbitals, and are nearly all within 10 kJ mol^{-1} of the MCSCF energies calculated with the same active space. Agreement between relative energies calculated by different methods is poor in some cases, with the worst conflict the 75 kJ mol^{-1} discrepancy between relative energies of the cyclic H_5C_4 evaluated at CISD and at MCSCF(9,9) levels. The other principal disagreement is a 20−40 kJ mol^{-1} offset of the multireference energies predicted for the radicals of 1,3-butadiene (HC_3HCH_3 and H_2C_2HCHCH) from the single-reference energies.

Several fundamental conclusions regarding the relative energies are supported by all the post-SCF calculations:

(1) Configuration 1 of $H_3C_4H_2$ is the most stable form of C_4H_5, and configuration 2 is not a stationary point on the surface.

(2) The HC_3HCH_3 forms 3a and 3b constitute resonance structures and not distinct isomers, despite their having different parent molecules. The staggered conformer lies between 9 and 15 kJ mol^{-1} higher in energy than $H_3C_4H_2$, with the eclipsed conformer, a saddle point on the surface, approximately 1 kJ mol^{-1} higher still.

(3) The $HC_3H_2CH_2$ structure lies some 50−70 kJ mol^{-1} above $H_3C_4H_2$.

(4) Configuration 4 of $H_2C_3HCH_2$ is the lowest energy isomer of the 1,3-butadiene daughter radicals, and the third or fourth lowest energy configurational isomer overall. Configuration 5 is significantly higher in energy, and corresponds to either a saddle point or an extremely shallow local minimum on the surface.[35]

(5) The H_2C_2HCHCH isomer lies 7−9 kJ mol^{-1} higher than configuration 5 of $H_2C_3HCH_2$.

Qualitative justifications for the relative stabilities of these isomers are consistent with the results from any post-SCF method. The isomers with allylic (three electron, three atom) conjugated systems are the most stable ($H_3C_4H_2$, HC_3HCH_3, and $HC_3H_2CH_2$ 4), followed by the structures with two conjugated π-bonds ($HC_3H_2CH_2$ 5 and H_2C_2HCHCH), and finally the unconjugated $HC_3H_2CH_2$ configuration. The cyclic structure has the stabilizing influence of an allylic electron distribution and an additional σ-bond, but these are balanced by the considerable ring strain.

Examination of the structures drawn in Figure 1 shows that the best agreement among predicted relative energies is for those structures with the most similar electron distributions. Consistent relative energies are predicted between the butynyl structures $H_3C_4H_2$ and HC_3HCH_3, and between the dienyls $^2A'$ $H_2C_3HCH_2$ and H_2C_2HCHCH, because these pairs have fundamental structural similarities. The $HC_3H_2CH_2$ radicals resemble $H_3C_4H_2$ and $HC_3H_2CH_2$ in having the butyne carbon chain, and the single- and multireference methods agree well in this case. On the other hand, the relocalization to transform the $^2A''$ state of $H_2C_3HCH_2$ to the $^2A'$ state involves substantial changes in the electron distribution, and the predicted energy gap of this pair ranges from roughly 20 to 50 kJ mol^{-1}. Similarly, the cyclic structure is unique in having a three-electron π-system, rather than the four and five-electron π-systems of the other species.

An obvious reason for poor agreement between single- and multireference methods is spin contamination of the single-reference wave functions. The expectation values $\langle S^2\rangle$ are reported in Table 5 for each configuration before and after annihilation of the spin contaminant, and indeed the values range from low contamination (0.75 for $HC_3H_2CH_2$) to high (1.18 for H_2C_2HCHCH), even after annihilation. The states with highest spin contamination are those with greatest population in the virtual UHF natural orbitals (UNOs). Table 5 shows that the $H_2C_3HCH_2$ and H_2C_2HCHCH radicals, which have $\langle S^2\rangle$ values over 0.84 after annihilation, all have orbital 16 populations of over 0.1, and have populations of over 3×10^{-4} for virtual orbitals as high as 24. Although the cyclic structure does not

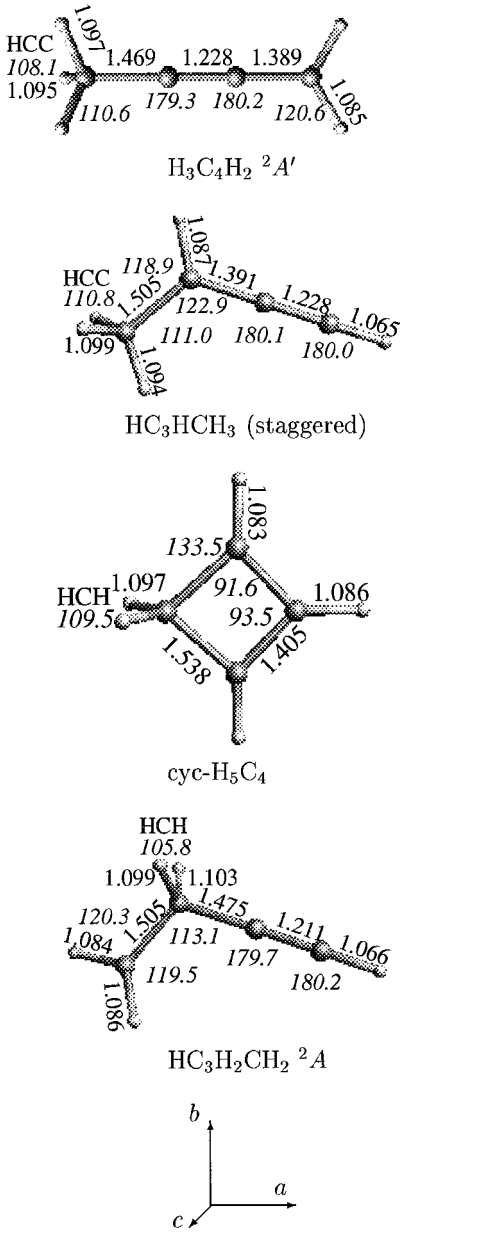

Figure 2. QCISD/6-311G(d,p) optimized geometries of selected isomers. Bond lengths are in Å, angles in degrees.

have such high spin contamination ($\langle S^2 \rangle = 0.76$ after annihilation), the borrowing of population by high-energy virtual UNOs exceeds that of $H_3C_4H_2$, HC_3HCH_3, and $HC_3H_2CH_2$.

The values of C_0^2 cited in Table 5 give the fractional contribution of the reference UHF function to the overall MCSCF(9,9) density. Although a low C_0^2 value suggests an inadequate reference function, single and double substitutions are normally sufficient to account for nearly all the remaining multireference density in the ground state. In these cases, C_0^2 is not an indicator of agreement between single- and multireference energies. The lowest values of C_0^2 are for $H_2C_3HCH_2$ 4, for which the difference between QCISD and MCSCF(9,9) energies is 35 kJ mol^{-1}, and for HC_3HCH_3, for which the difference is only 3 kJ mol^{-1}.

Equilibrium geometries and vibrational frequencies agree well across all post-SCF levels of theory. In particular, the large discrepancy between cyclic H_5C_4 relative energies predicted by single- and multireference methods does not manifest similar discrepancies for other properties. All cyclic H_5C_4 bond lengths predicted at QCISD and MCSCF(9,9) levels differ by less than 0.015 Å, and the bond angles by less than 1.1°, differences significantly less than the expected zero-point oscillations (>0.04 Å for C−C stretches, ≈ 0.10 Å for C−H stretches). Variability among the QCISD and MCSCF(9,9) predicted vibrational frequencies is 7% or less, excepting the lowest frequency mode for which the QCISD predicted frequency is 358 cm^{-1} and the MCSCF(9,9) value is 398 cm^{-1}. Discrepancies between QCISD and CISD predicted frequencies are slightly smaller, typically 5% or less.

TABLE 6: Selected Spectroscopic Properties for C_4H_5 Isomers at the QCISD Level

	$H_3C_4H_2$ (1) $^2A'$	HC_3HCH_3 (3) stag	cyc-H_5C_4 $^2A_2$	$HC_3H_2CH_2$ $^2A''$
	Rotational Constants (cm^{-1})			
A	3.416	1.268	0.472	1.041
B	0.118	0.146	0.433	0.156
C	0.117	0.134	0.236	0.139
	Dipole Moments (D)[a]			
μ_a	−0.743	−0.465	−0.022	−0.484
μ_b	0	−0.069	0	0.270
	Frequencies (cm^{-1}) and Intensities (km mol^{-1}) of the Strongest Vibrational Modes			
	603(46)	447(59)	521(73)	290(21)
	2164(20)	656(45)	1015(12)	368(29)
	3054(26)	3036(27)	3068(39)	651(41)
	3121(13)	3089(22)	3115(30)	676(40)
	3132(12)	3484(52)	3245(15)	3491(50)

[a] Dipole components along principal inertial axes, oriented as drawn in Figure 2. All *c*-axis components are zero.

The dramatic efficiency and accuracy of the B3LYP density functional method has led to its rapid application to a wide variety of molecular computations. The method fails in the present case to accurately predict the relative energy of the cyclic isomer, but fares well otherwise. Bond lengths predicted at the QCISD and B3LYP levels agree to within 0.028 Å; bond angles agree to within 1.2°; and vibrational frequencies to within 90 cm^{-1} for the CH stretches and (with few exceptions) within 50 cm^{-1} for other modes. This is generally better agreement than is found between the MP2 and QCISD results, which include disparities in the vibrational frequencies as large as 200 cm^{-1}.

In general we will cite QCISD-calculated properties, because the available experimental hyperfine parameters and energies are in excellent agreement with the QCISD predictions. The QCISD optimized geometries of the most stable conformers are drawn in Figure 2. The overestimated multireference energies indicate that the dynamical correlation energy contributions vary too much among these structural isomers for adequate modeling by CI substitutions of only the highest nominally occupied orbitals.

Rotational constants, dipole moments, and properties of the five strongest vibrational modes calculated at the QCISD level are reported in Table 6 for four of the six structural isomers in their most stable conformations. Properties for H_2C_2HCHCH and $H_2C_3HCH_2$ have been previously reported.[35]

3.1. $H_3C_4H_2$. This structural isomer, obtained by removal of a hydrogen from 2-butyne or by removal of the 2-hydrogen from 1,2-butadiene, is predicted to be the most stable structural isomer of C_4H_5 at all levels of theory. This isomer is also found to be the lowest energy structure in calculations by Kühnel[24,25] and Somasundram.[34] Only configuration 1, with the linear C_4 chain, is found to be a minimum on the UHF, QCISD, and MCSCF-(9,9) potential surfaces for the ground electronic state. The bent configuration 2 of this structure is not a stationary point on either the $^2A'$ or $^2A''$ potential energy surfaces, deforming without

barrier to configuration 1. The surfaces of both A' and A'' symmetries were considered, because the unpaired electron in configuration 2, as drawn in Figure 1, may be localized in either an in-plane sp^2 hybrid orbital (for $^2A'$) or in an out-of-plane p orbital (for $^2A''$). Both electron configurations are similar in energy, to the extent that the $^2A''$ is the ground state of the structurally similar H_3C_3O radical[30] while the $^2A'$ surface is found to be more stable for $H_3C_4H_2$.

The stability of this isomer compared to other C_4H_5 isomers is consistent with the findings of Nguyen and King, who determined a formation enthalpy of 303 kJ mol^{-1} for this isomer based on the decomposition threshold of 3-methylbut-1-yne,[1] later lowering the value to 294 kJ mol^{-1}, based on the decomposition threshold of 2-pentyne.[2] A previous value of 308 kJ mol^{-1} had been determined in shock tube studies by Tsang,[53] but a more recent measurement of the propene bond dissociation energy[54] (BDE) adjusts this enthalpy to 293 kJ mol^{-1}. From Nguyen and King's measurements and a 145.7 kJ mol^{-1} formation enthalpy of 2-butyne, the current accepted value of $\Delta_f H^\ominus$ for $H_3C_4H_2$ is 295.0(9.2) kJ mol^{-1} at 300 K. We estimate the formation enthalpy of $H_3C_4H_2$ at the QCISD level by calculation of the C_2H_2 and atomic hydrogen energies using unrestricted reference wavefunctions. Including zero-point corrections, the reaction enthalpy for formation of $H_3C_4H_2$ from $2C_2H_2 + H$ is predicted to be -392 kJ mol^{-1}, which (using standard formation enthalpies for the reactants) leads to a calculated $H_3C_4H_2$ formation enthalpy of 280 kJ mol^{-1}, roughly 15 kJ mol^{-1} lower than the experimental value.

The geometry in Figure 2 is generally consistent with canonical structure 1a drawn in Figure 1. The carbon−carbon bond lengths predicted from a standard table[55] are 1.46 Å for the C_aC_b bond, and 1.20 and 1.45 Å for the remaining formal triple and single bonds, respectively. Resonance form 1b has formal C_bC_c and C_cC_d double bonds, predicting bond lengths of 1.46, 1.28, and 1.31 Å, respectively. The calculated equilibrium geometry represents an average of the two structures, with emphasis on the alkyne form. Evidence for contributions from both resonance forms was found in branching of reactions between methyl radical and $H_3C_4H_2$ in the 1980 study by Deschênes and co-workers.[10]

Although configuration 2 of $H_3C_4H_2$ is not a minimum on the potential energy surface, its geometry is relatively low in energy, giving the lowest carbon-chain bending vibration a harmonic frequency of only 167 cm^{-1}. The QCISD potential energy surface along this bending coordinate was sampled by fixing the $C_aC_bC_c$ bond angle in 10° increments while optimizing all other geometric parameters, giving the curve drawn in Figure 3. At a bond angle of 140°, 40° different from the equilibrium angle, the energy has risen by only 27 kJ mol^{-1}. This is consistent with the 23 kJ mol^{-1} relative energy estimated from the formation enthalpy of 1,2-butadiene and the BDE of allene.[56]

The shape of this potential contrasts with that of the analogous H_3C_3O molecule, obtained by replacing the $H_3C_4H_2$ methylene group with an oxygen atom. The equilibrium geometry of H_3C_3O is bent at the QCISD and MCSCF levels,[30] with a CCC bond angle of about 150°. The H_3C_3O molecule, unlike $H_3C_4H_2$, is subject to Jahn−Teller distortion, because at the C_{3v} geometry attained when the C_3O chain is straight, the ground electronic state has degenerate E symmetry. Consequently, the C_3O chain stabilizes by bending to a C_s geometry with a non-degenerate $^2A''$ state. Replacement of the O atom with CH_2 breaks the degeneracy of the ^2E electronic state, nullifying the Jahn−Teller effect. The C_4 chain is more stable when straight, allowing delocalization of the unpaired electron through the allylic system

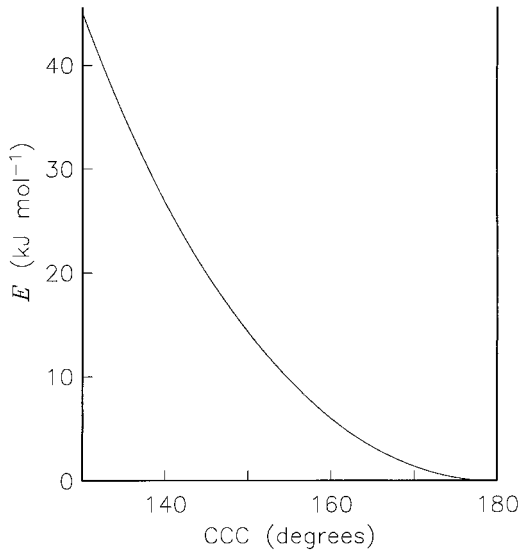

Figure 3. Potential energy as a function of the $C_aC_bC_c$ bending angle of $H_3C_4H_2$, evaluated at the QCISD/6-311G(d,p) level.

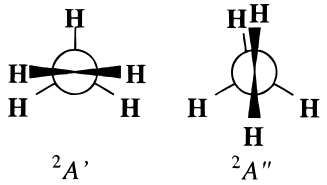

Figure 4. The two C_s conformers of $H_3C_4H_2$.

of configuration 1, rather than localizing the electron in the manner suggested by configuration 2. The QCISD Mulliken spin densities indicate that the methylene carbon C_d bears most of the unpaired electron density, 0.96 compared to 0.54 for C_b.

Internal rotation of the $H_3C_4H_2$ methyl group is essentially unhindered, as is expected given the 4 Å separation between methyl and methylene groups. Less than a 0.5 kJ mol^{-1} difference is found between stabilization energies of the $^2A'$ and $^2A''$ conformers (Figure 4) at all levels of theory, with the $^2A'$ always slightly more stable. Harmonic frequency analyses at the $^2A'$ and $^2A''$ conformational geometries uniformly predict the $^2A'$ structure to be a minimum energy geometry, but give mixed results as to whether the $^2A''$ conformer is a local minimum or a saddle point. The potential surface along this torsional coordinate was tested at the QCISD level by evaluating energies at fixed geometries for 10° intervals, and a barrier of only 0.012 kJ mol^{-1} is found. The distinction between secondary minimum and saddle point has little experimental significance for so flat a potential. Very low force constants are found, as expected for a nearly free rotor. At the QCISD level, the harmonic frequency for the internal rotation is predicted to be 17 cm^{-1} for the $^2A'$ conformer, and 7 cm^{-1} for the $^2A''$ conformer. Free methane has a rotational constant of 5.3 cm^{-1}. The remaining QCISD frequencies for the $^2A''$ conformer differ from those of the $^2A'$ by less than 1.5 cm^{-1}, and the optimized geometries differ by less than 0.001 Å in bond lengths and 0.6° in bond angles.

Support for the accuracy of the predicted electron distribution is provided by the hyperfine constants. The proton hyperfine parameters determined by the recent ESR spectra of Tachikawa and co-workers[21] are in good agreement with the Fermi contact terms predicted at the QCISD level, as shown in Table 7. Previous measurements of these parameters by Ohta et al. and MacInnes and Walton differ from Tachikawa's by 0.6 MHz or less.[19,20] The very low barrier to methyl rotation is consistent

TABLE 7: Experimental and QCISD Fermi Contact Parameters (MHz)[a]

$H_3C_4H_2$		HC_3HCH_3		cyc-H_5 C_4		$H_2C_3HCH_2$	H_2C_2HCHCH
calcd	expt[21]	calcd	expt[21]	calcd	expt[22]	calcd	calcd
27.9	35.0	47.8	52.1	15.5	12.4	−51.9	28.2
27.9	35.0	47.8	52.1	15.5	12.4	−50.2	135.3
27.9	35.0	47.8	52.1	−52.1	−42.5	14.3	−0.8
−62.3	−52.1	−62.6	−52.1	−52.1	−42.5	83.0	0.1
−62.3	−52.1	−38.0	−33.6	10.6	6.7	83.0	−0.4

[a] Signs of the experimental values have been set to those determined from ab initio results. Hydrogens are listed according to the atom labels in Figure 1, ordered first by the corresponding carbon atom label (C_a, C_b, C_c, C_d), and then (for nonequivalent hydrogens bonded to the same atom) by hydrogen atom labels.

with experimental observation of a single hyperfine constant for the three methyl protons, even at 77 K.[21] Because the hyperfine constants are predicted only for rigid conformations, the calculated values of the Fermi contact term are arithmetic averages of the values predicted for the $^2A'$ and $^2A''$ conformers.

The experiment determines magnitudes but not signs for the hyperfine parameters, and we have therefore fixed the signs of the experimental values in Table 7 to those determined in the calculations. Those signs are consistent with previous INDO predictions,[21] and with expectations. The Fermi contact term *a* is proportional to the spin density at the nucleus, $|\psi(0)|^2$, and is therefore often used as an indicator of unpaired electron s character at that nucleus. The nuclear magnetic moment of the proton is positive, and s-type electron spin density at the proton leads to a positive value of *a*. For example, the predicted Fermi contact term for the H atom adjacent to atom C_a in H_2C_2HCHCH is 28 MHz, and is attributable to spillover of the C_a sp^2 hybrid orbital of the unpaired electron onto the proton. If the unpaired electron is constrained by symmetry to have no s character at the proton, then the spin polarization dominates the Fermi contact term. In particular, an out-of-plane p orbital with high spin density at a carbon atom tends to repel the like-spin electron density at an adjoining hydrogen atom. This gives a net spin density at the proton, but with spin opposite to that of the unpaired electron, and the Fermi contact term is then negative. This accounts for the negative *a* values predicted for the two equivalent protons in $H_3C_4H_2$.

3.2. HC_3HCH_3. The HC_3HCH_3 radical is obtained by abstraction of either the 3-hydrogen from 1-butyne or the 1-hydrogen from 1,2-butadiene. This isomer lies less than 16 kJ mol^{-1} higher than $H_3C_4H_2$ according to every level of theory used, consistent with Somasundram's MP3/6-31G(d) relative energy of 13.0 kJ mol^{-1}.[34] The experimental value of 2.4 kJ mol^{-1} is obtained using Nguyen and King's 1981 formation enthalpy for HC_3HCH_3 and their 1982 formation enthalpy for $H_3C_4H_2$.[1,2] An allylic electron distribution is again a likely contributor to the stability of this structure over its nonallylic isomers.

Structures 3a and 3b in Figure 1 are resonance structures of a single observable geometry; no secondary minimum is found, for example, for a sp^2 hybrid geometry of the C_d bonds. The CC bond lengths predicted at the QCISD level are 1.505, 1.391, and 1.228 Å, and the carbon atom Mulliken spin densities are −0.09, 0.91, −0.36, and 0.54 for atoms C_a, C_b, C_c, and C_d, respectively. These results are consistent with configuration 3a being mixed with a small contribution from configuration 3b.

Torsion of the methyl group is more hindered by the bent carbon chain in HC_3HCH_3 than by the distant methylene group in $H_3C_4H_2$, but the interaction is still weak. The conformer with an eclipsed C_2H group (Figure 5) lies roughly 1 kJ mol^{-1} higher in energy than the staggered conformer, according to the CI and MCSCF calculations. However, the QCISD potential surface is quite flat along this coordinate, and numerical frequency analysis at the equilibrium geometry mistakenly reports a small negative force constant (−0.0002 mdyne/Å). Fixed geometry calculations verify that small displacements along this coordinate only increase the potential energy.

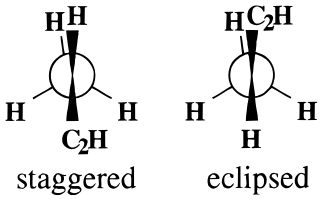

Figure 5. The two C_s conformers of HC_3HCH_3.

Optimized geometries of the staggered and eclipsed conformer differ by less than 0.4 Å and 1.1° at the QCISD level. As indicated by square brackets around the zero-point corrected energies in Table 2, the staggered geometry is found to be a saddle point, not a local minimum, at the MP2 and MCSCF-(7,7) levels. However, the optimized geometries at these levels differ from the optimized C_s staggered geometries only by 2° internal rotations of the methyl group. The distinction is likely to arise from a minor symmetry instability in those calculations, and the predicted relative energies and spectroscopic parameters are not significantly affected.

Experimental hyperfine parameters[21] are again available for comparison in Table 7, and values agree to within 11 MHz. Again, the single value cited for the methyl protons estimates the observed, internal rotation-averaged value by an arithmetic average of ab initio values for the rigid staggered and eclipsed conformations. Signs of the experimental values are again fixed by the calculations, and are consistent with spin polarization from unpaired electron density at atoms C_b and C_d reversing the sign of *a* at the adjacent hydrogens.

3.3. Daughter Radicals of 1,3-Butadiene. We have previously reported that configuration 4 of $H_2C_3HCH_2$ (a $^2A''$ state) is predicted at the UHF, B3LYP, QCISD, CCSD(T), and MCSCF(9,9) to be the most stable of the 1,3-butadiene daughter radicals.[35] Configuration 5 of that structure (a $^2A'$ state) was found to be a saddle point in the single-reference calculations and a very shallow minimum at the MCSCF level, higher in energy than 4 by 25−35 kJ mol^{-1}. The H_2C_2HCHCH structure was found to be a local minimum in any of four possible cis/trans configurations, with the trans-trans configuration discussed in the present work always the most stable. The *tt*-H_2C_2HCHCH configuration consistently lies roughly 10 kJ mol^{-1} higher in energy than configuration 5 at several levels of theory.

The present work extends these results to MP, CISD, and additional multi-reference levels, and the findings are consistent with previous conclusions. Across all post-SCF levels of theory used, the energy gap between $H_2C_3HCH_2$ 5 and *tt*-H_2C_2HCHCH ranges from 6.6 to 12.3 kJ mol^{-1}.

The gap between $H_2C_3HCH_2$ 4 and *tt*-H_2C_2HCHCH is not so consistent, ranging from 57.9 kJ mol^{-1} at the MP3 level down to 22.4 kJ mol^{-1} at the MCSCF(7,7) level. The previous literature contains relative energies for $H_2C_3HCH_2$ and H_2C_2-HCHCH which appear to be based primarily on the $^2A''$ configuration 4 of the former.[35] These consistently predict a relative energy of 31 to 42 kJ mol^{-1}, whether determined by group additivities[8] or ab initio calculations.[12,42] This range is in fair agreement with the coupled cluster energies (39.9 and 43.4 for CCSD(T) and QCISD, respectively), but is better matched

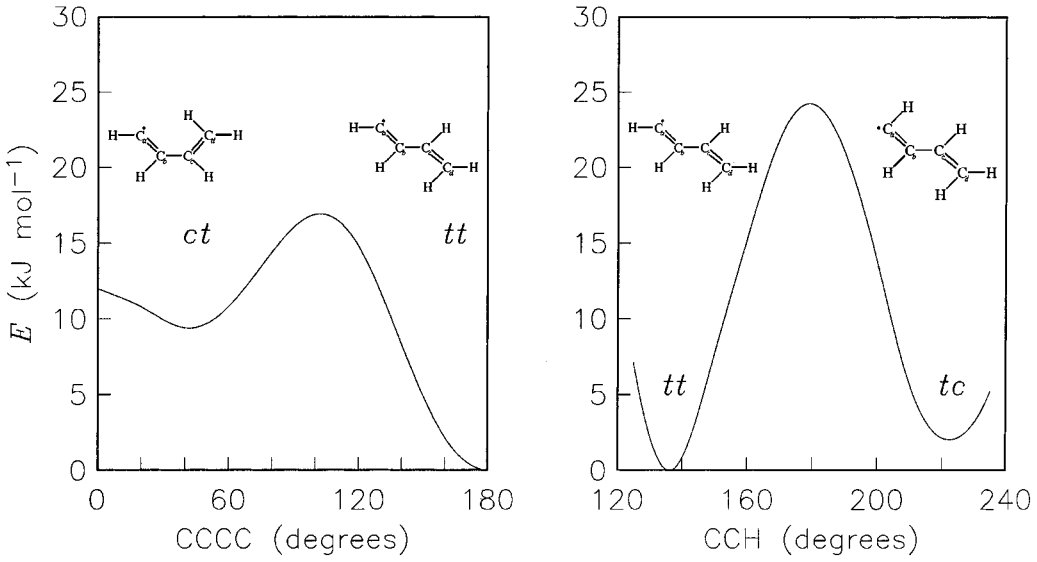

Figure 6. QCISD potential energy curves for conformational isomerizations of H_2C_2HCHCH.

by the higher order MRCISD energies, such as the 34.1 kJ mol^{-1} difference predicted at the MRCISD(7,7,43) level.

The empirical relative energies in Table 2 are based on the known BDE of 1,2-butadiene[57] to form $H_2C_3HCH_2$ 4, and on a BDE to form *tt*-H_2C_2HCHCH from 1,3-butadiene estimated from the 465.3(3.4) kJ mol^{-1} BDE of ethene.[54,58] While relative energies within this group are adequately predicted by either single- or multireference methods, it appears that the MCSCF calculations significantly overestimate the energies relative to $H_3C_4H_2$. Despite the very high spin contamination, the QCISD relative energies are more reliable. Experimental determination of the hyperfine constants predicted in Table 7 for the *tt* form will further ascertain the accuracy of the single-reference calculations.

The potential energy curves for isomerization between the *tt* and two other minimum energy conformations are shown in Figure 6. The *ct* conformer is obtained from the *tt* by rotation about the central C−C bond, resulting in cis double bonds. The *ct* conformer corresponds to a non-planar local minimum (C_4 dihedral angle = 41.3°) on the QCISD surface 9.4 kJ mol^{-1} higher in energy than the *tt* conformer, separated by a barrier of about 17 kJ mol^{-1} at a dihedral angle of about 100°. The *tc* conformer is obtained from the *tt* by in-plane motion of the terminal hydrogen atom from a CCH bond angle of 136.0° to 224.0°, resulting in a cis orientation of the terminal hydrogen to the central C−C bond. The barrier for this motion is shown to be roughly 25 kJ mol^{-1} at 180°. An investigation of C_1 geometries confirms that the in-plane motion is the lowest energy path, as this does not disturb the conjugation of the π-bonds. Because the *tt* and *tc* isomers differ in energy by only 2.4 kJ mol^{-1}, and the *ct* and *cc* isomers by less than 0.1 kJ mol^{-1}, it is likely that the analogous isomerizations involving the *cc* isomer have similar barriers. These barriers are all high enough to support bound vibrational states, and it is likely that all four of the conformations of H_2C_2HCHCH are experimentally observable.

3.4. Cyclic H_5C_4. This, the only cyclic isomer investigated in detail in the present work, presents the most significant disagreement among levels of theory. At the QCISD and CCSD(T) levels of theory, the relative energy of this isomer is 11−12 kJ mol^{-1}. At MCSCF levels, the relative energy is about 80 kJ mol^{-1}, the highest among the isomers studied.

The empirical energy reported in Table 2 is an estimate using the 156.7 kJ mol^{-1} enthalpy of formation of cyclobutene and the 361.9(8.8) kJ mol^{-1} BDE of propene.[54] Propene should be an accurate model of the cyclobutene BDE, because it too loses a hydrogen atom to form an allyl-stabilized radical. Hydrogen abstraction from cyclobutane to form cyclobutyl radical involves no such stabilization, and the 403.8 kJ mol^{-1} BDE of cyclobutane[57] predicts a firm upper limit to the cyclobutenyl relative energy of 50.0 kJ mol^{-1}, still 25 kJ mol^{-1} less than the MCSCF values. This strongly favors the single-reference CI and CC results over the multireference results.

As a cyclic structure, cyclobutenyl has one more σ-bonding orbital than the other isomers, and one less orbital in the π-system. To estimate the nondynamical correlation energy of the molecule by multireference calculations, one would typically choose a (3,3) active space using the doubly and singly occupied π orbitals and the lowest unoccupied π orbital. However, the UNO populations in Table 5 indicate that populations of occupied orbitals well outside the active spaces used in our work vary slightly from the cyclic to other isomers. At the relevant energy scale of about 10 kJ mol^{-1}, the dynamical correlation energy contributions arising from CI substitutions out of these orbitals may differ enough among the isomers to account for the observed discrepancy.

While we tentatively ascribe the difference in predicted energies to the neglect of CI substitutions from low-energy valence orbitals, it is surprising that this relative energy is fairly insensitive to size of the active space, unlike the 1,3-butadiene radical energies. We note that Olivella and Solé's study of the bicyclobutyl ring-opening isomerization to cyclic H_5C_4 found that MCSCF methods gave reasonable geometries but energies in error by 40−50 kJ mol^{-1}.[28]

Hyperfine parameters evaluated at the QCISD level are in excellent agreement with experiment, as shown in Table 7. All predictions lie within 10 MHz of the magnitudes determined by ESR.[22]

3.5. $HC_3H_2CH_2$. This radical may be formed by removal of a 4-hydrogen from 1,2-butadiene. All methods concur that this structure has two minimum energy conformers: the $^2A'$ C_s eclipsed form and a ^2A C_1 form, for which the terminal CH_2 group is rotated about 25° about the CC single bond from the C_s staggered geometry (Figure 7). Properties were also evaluated for a third conformer, a saddle point at a second C_s geometry having $^2A'$ symmetry. These three conformers vary in energy by 1.4−2.6 kJ mol^{-1} (Table 3) and differ in bond lengths and angles by less than 0.005 Å and 1.1°, respectively. Prior to zero-

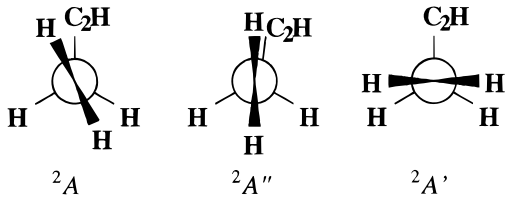

Figure 7. The conformers of $HC_3H_2CH_2$.

point corrections, the C_1 conformer is always found to be the most stable, and is the only minimum energy asymmetric geometry identified for these six C_4H_5 structural isomers. However, addition of the zero-point corrections shifts the relative energies such that the $^2A''$ conformer becomes the most stable, followed by the ^2A and $^2A'$ conformers in that order. (Only at the MP2 level is the order different, with $^2A'$ the most stable conformer and ^2A the least.)

The relative energy is estimated in Table 2 by using the 420.0-(2.5) BDE of $H-CH_2CH_2CH_3$ to approximate the BDE of $H-CH_2CH_2CCH$. This empirical value overestimates the relative energy, because the ethynyl group CCH weakens neighboring C−H bonds more than the methyl group, and this estimated value of 75 kJ mol^{-1} is higher than the QCISD prediction by roughly 1.5 times the experimental uncertainty in the BDE.

This structure essentially lacks orbital conjugation, as the two π-bonds are mutually perpendicular and the unpaired electron is adjacent to neither. Consequently, Table 5 shows that the spin contamination is very low and effectively removed by annihilation, the reference state comprises 90% of the MCSCF(9,9) density, and the UNO populations are almost entirely confined to the nominally occupied orbitals.

4. Conclusions

This work completes our investigation of the most stable C_4H_5 isomers. Predicted relative energies of the $H_3C_4H_2$, HC_3HCH_3, and HC_3HCH_3 structural and conformational isomers are consistent across several CI, CC, MCSCF, and MRCISD levels, as are the predicted relative energies within the group of 1,3-butadiene daughter radicals. Discrepancies between these two series are tentatively attributed to the neglect of CI substitutions from low-energy valence orbitals by the multireference wave functions, and hence relatively poor accuracy in assessing the relative dynamical correlation energies. This is consistent with the continued decline of MCSCF energies for $H_2C_3HCH_2$ and H_2C_2HCHCH on expansion of the active space, and with the experimental relative energies in Table 2.

Predicted values for relative conformational energies, vibrational frequencies, and equilibrium geometries are consistent across several levels of theory. The QCISD calculations predict the empirical relative energies within measured or estimated errors, and the QCISD spin density accurately predicts the observed hyperfine parameters for the three structures for which experimental data is available. Of eight distinct proton hyperfine constants measured, all agree with predicted values within 11 MHz, and half are within 5 MHz.

For various reasons, the relocalization pathways that so dramatically affect the vibrational surfaces of the C_3H_3O isomers do not play a central role in shaping the surfaces of these species. Two of the C_3H_3O isomers that exhibited multiple minima, H_2C_2HCO and H_2C_3HO, are analogous to the same C_4H_5 structural isomer, $H_2C_3HCH_2$. The $H_3C_4H_2$ radical in the present study is analogous to H_3C_3O. The role of the allylic conjugation that stabilizes configuration 4 relative to configuration 5 of $H_2C_3HCH_2$ and configuration 1 relative to configuration 2 of $H_3C_4H_2$ is offset in the C_3H_3O isomers by the higher electronegativity of the oxygen atom. The higher electronegativity favors canonical forms that localize unbonded electrons on atoms adjacent to the oxygen, while discouraging those that violate the octet rule for oxygen. This tends to equalize energies among distinct configurations in the C_3H_3O series, leading to flatter ab initio surfaces.

The $H_3C_4H_2$, HC_3HCH_3, and $HC_3H_2CH_2$ radicals each are predicted to have dipole moment components in excess of 0.45 D, and their rotational spectra should be observable by existing Fourier transform microwave techniques.[59] The cyclic structure presents a greater challenge, having only a 0.022 D predicted dipole moment. Vibrational spectra of these radicals lack the very strong stretching modes of the C_3H_3O isomers, and are limited to band intensities of under 80 km mol^{-1}. The strongest modes are generally low-frequency bending modes that substantially distort the molecule or C−H stretching modes, particularly of the ethynyl hydrogen bonds in HC_3HCH_3 and $HC_3H_2CH_2$. These may be well-suited to study by matrix-isolation spectroscopy, using photolysis of precursor halocarbons as a production scheme.

Acknowledgment. These calculations were carried out partly at the Mississippi Center for Supercomputing Research. The authors thank D. Southard for assistance and Dr. N. C. Handy for kindly supplying a copy of reference 34. This work was funded by the National Science Foundation and by the Exxon Education Foundation. Acknowledgment is also made to the donors of the Petroleum Research Fund, administered by the ACS, for partial support of this research.

Supporting Information Available: Complete tables of QCISD/6-311G(d,p) harmonic vibrational frequencies and intensities for all optimized stationary points studied. This material is available free of charge via the Internet at http://pubs.acs.org.

Registry No. (Supplied by Author): $H_3C_4H_2$ 1a, 82252-88-8; 1b and 2, 78901-40-3; HC_3HCH_3 3a, 3315-42-2; 3b, 4777-46-2; $H_2C_3HCH_2$ 4, 89829-51-6; 5, 108179-96-0; c-H_5 C_4, 24669-29-2; H_2C_2HCHCH, 86181-68-2; $HC_3H_2CH_2$, 108179-95-9.

References and Notes

(1) Nguyen, T. T.; King, K. D. *J. Phys. Chem.* **1981**, *85*, 3130−3136.
(2) Nguyen, T. T.; King, K. D. *Int. J. Chem. Kinet.* **1982**, *14*, 613−621.
(3) Trenwith, A. B.; Wrigley, S. P. *J. Chem. Soc., Faraday Trans. 1* **1982**, *78*, 2337−2347.
(4) Cole, J. A.; Bittner, J. D.; Longwell, J. P.; Howard, J. B. *Combust. Flame* **1984**, *56*, 51−70.
(5) Weissman, M.; Benson, S. *Int. J. Chem. Kinet.* **1984**, *16*, 307−333.
(6) Weissman, M.; Benson, S. *J. Phys. Chem.* **1988**, *92*, 4080−4084.
(7) Durán, R. P.; Amorebieta, V. T.; Collusi, A. J. *J. Phys. Chem.* **1988**, *92*, 636−640.
(8) Kern, R. D.; Singh, H. J.; Wu, C. H. *Int. J. Chem. Kinet.* **1988**, *20*, 731−747.
(9) Westmoreland, P. R.; Dean, A. M.; Howard, J. B.; Longwell, J. P. *J. Phys. Chem.* **1989**, *93*, 8171−8180.
(10) Deschênes, J.; Deslauriers, H.; Collin, G. J. *Can. J. Phys.* **1980**, *58*, 2108−2114.
(11) Callear, A. B.; Smith, G. B. *Chem. Phys. Lett.* **1984**, *105*, 119−122.
(12) Callear, A. B.; Smith, G. B. *J. Phys. Chem.* **1986**, *90*, 3229−3237.
(13) Kaiser, R. I.; Stranges, D.; Lee, Y. T.; Suits, A. G. *Astrophys. J.* **1997**, *477*, 982−989.
(14) Martin, M. M.; Sanders, E. B. *J. Am. Chem. Soc.* **1967**, *89*, 3777−3782.
(15) Benson, S. W.; Haugen, G. R. *J. Phys. Chem.* **1967**, *71*, 1735−1746.

(16) Marinov, N. M.; Pitz, W. J.; Westbrook, C. K.; Vincetore, A. M.; Castaldi, M. J.; Senkan, S. M.; Melius, C. F. *Combust. Flame* **1998**, *114*, 192−213.
(17) Krusic, P. J.; Jesson, J. P.; Kochi, J. K. *J. Am. Chem. Soc.* **1969**, *91*, 4566−4568.
(18) Lunazzi, L.; Placucci, G.; Grossi, L. *J. Chem. Soc., Perkin Trans. 2* **1980**, *7*, 1063−1066.
(19) MacInnes, I.; Walton, J. C. *J. Chem. Soc., Perkin Trans. II* **1987**, 1077−1082.
(20) Ohta, K.; Shiotani, M.; Sohma, J.; Hasegawa, A.; Symons, M. C. R. *Chem. Phys. Lett.* **1987**, *136*, 465−470.
(21) Tachikawa, H.; Shiotani, M.; Ohta, K. *J. Phys. Chem.* **1992**, *96*, 164−171.
(22) Barone, V.; Adamo, C.; Grand, A.; Subra, R. *Chem. Phys. Lett.* **1995**, *246*, 53−58.
(23) Kaiser, R. I.; Stranges, D.; Bevsek, H. M.; Lee, Y. T.; Suits, A. G. *J. Chem. Phys.* **1997**, *106*, 4945−4953.
(24) Kühnel, W.; Gey, E.; Ondruschka, B. Z. *Z. Phys. Chem. (Leipzig)* **1987**, *268*, 23−32.
(25) Kühnel, W.; Gey, E.; Ondruschka, B. Z. *Z. Phys. Chem. (Leipzig)* **1987**, *268*, 805−814.
(26) Wang, H.; Frenklach, M. *J. Phys. Chem.* **1994**, *98*. 11465−11489.
(27) Pacanski, J.; Yoshimine, M. *J. Phys. Chem.* **1985**, *89*, 1880−1883.
(28) Olivella, S.; Sole, A. *J. Am. Chem. Soc.* **1991**, *113*, 87−94.
(29) Barone, V.; Subra, R. *J. Chem. Phys.* **1996**, *104*, 2630−2637.
(30) Cooksy, A. L. *J. Phys. Chem.* **1998**, *102*, 5092−5099.
(31) Cooksy, A. L. In preparation.
(32) Cooksy, A. L.; Tao, F.-M.; Klemperer, W.; Thaddeus, P. *J. Phys. Chem.* **1995**, *99*, 11095−11100.
(33) Wang, H.; Cooksy, A. L. *Chem. Phys.* **1996**, *213*, 139−151.
(34) Somasundram, K. Thesis, University of Cambridge, 1987.
(35) Parker, C. L.; Cooksy, A. L. *J. Phys. Chem.* **1998**, *102*, 6186−6190.
(36) Krishnan, R.; Binkley, J. S.; Seeger, R.; Pople, J. A. *J. Chem. Phys.* **1980**, *72*, 650−654.
(37) Frisch, M. J.; Pople, J. A.; Binkley, J. S. *J. Chem. Phys.* **1984**, *80*, 3265−3269.
(38) T. H. Dunning, J. *J. Chem. Phys.* **1989**, *90*, 1007−1023.
(39) Tao, F.; Pan, Y. K. *J. Chem. Phys.* **1992**, *97*, 4989−4995.
(40) Partridge, H.; Bauschlicher, C. W., Jr. *J. Chem. Phys.* **1998**, *109*, 4707−4712.
(41) Werner, H.-J. *Adv. Chem. Phys.* **1987**, *69*, 1−62.
(42) Shepard, R. *Adv. Chem. Phys.* **1987**, *69*, 63−200.
(43) Raghavachari, K.; Pople, J. A. *Int. J. Quantum Chem.* **1981**, *20*, 1067−1071.
(44) Pople, J. A.; Head-Gordon, M.; Raghavachari, K. *J. Chem. Phys.* **1987**, *87*, 5968−5975.
(45) Purvis, G. D., III; Bartlett, R. J. *J. Chem. Phys.* **1982**, *76*, 1910−1918.
(46) Becke, A. D. *J. Chem. Phys.* **1993**, *98*, 5648−5652.
(47) Lee, C.; Yang, W.; Parr, R. G. *Phys. Rev. B* **1988**, *37*, 785−789.
(48) Frisch, M. J.; Head-Gordon, M.; Pople, J. A. *Chem. Phys. Lett.* **1990**, *166*, 281−289.
(49) Pipek, J.; Mezey, P. Z. *J. Chem. Phys.* **1989**, *90*, 4916−4926.
(50) Krishnan, R.; Pople, J. A. *Int. J. Quantum Chem.* **1978**, *14*, 91−100.
(51) Schmidt, M. W., et al. *J. Comput. Chem.* **1993**, *14*, 1347−1363.
(52) Frisch, M. J., et al. *Gaussian 94*, Revision C; Gaussian, Inc.: Pittsburgh, 1994.
(53) Tsang, W. *Int. J. Chem. Kinet.* **1978**, *10*, 687−711.
(54) Berkowitz, J.; Ellison, G. B.; Gutman, D. *J. Phys. Chem.* **1994**, *98*, 2744−2765.
(55) Ladd, M. F. C.; Palmer, R. A. *Structure determination by X-ray crystallography*; Plenum Press: New York, 1985.
(56) Robinson, M. s.; Polak, M. L.; Bierbaum, V. M.; DePuy, C. H.; Lineberger, W. C. *J. Am. Chem. Soc.* **1995**, *117*, 6766−6778.
(57) McMillen, D. F.; Golden, D. M. *Ann. Rev. Phys. Chem.* **1982**, *33*, 493−532.
(58) Russell, J. J.; Senkan, S. M.; Seetula, J. A.; Gutman, D. *J. Phys. Chem.* **1989**, *93*, 5184−5188.
(59) Chen, W.; Novick, S. E.; McCarthy, M. C.; Travers, M. J.; Gottlieb, C. A.; Cooksy, A. L.; Thaddeus, P. *Astrophys. J.* **1996**, *462*, L561−L562.